World Journal of Gastroenterology

Submit a Manuscript: http://www.wjgnet.com/esps/
Help Desk: http://www.wjgnet.com/esps/helpdesk.aspx
DOI: 10.3748/wjg.v22.i11.3242

World J Gastroenterol 2016 March 21; 22(11): 3242-3251
ISSN 1007-9327 (print) ISSN 2219-2840 (online)

ORIGINAL ARTICLE

Retrospective Study

Application of gemstone spectral imaging for efficacy evaluation in hepatocellular carcinoma after transarterial chemoembolization

Qi-Yu Liu, Chuan-Dong He, Ying Zhou, Dan Huang, Hua Lin, Zhong Wang, Dong Wang, Jin-Qiu Wang, Li-Ping Liao

Qi-Yu Liu, Chuan-Dong He, Ying Zhou, Dan Huang, Hua Lin, Zhong Wang, Dong Wang, Jin-Qiu Wang, Li-Ping Liao, Department of Radiology, Mianyang Central Hospital, Mianyang 621000, Sichuan Province, China

Author contributions: Liu QY designed the research and wrote the paper; He CD designed the research and supervised the report; Zhou Y and Huang D contributed to the analysis; Lin H and Wang D provided clinical advice; Wang Z, Wang JQ and Liao LP performed the research.

Institutional review board statement: This study was reviewed and approved by the Ethics Committee of the Mianyang Central Hospital, Sichuan Province, China.

Informed consent statement: All patients provided written informed consent prior to GSI scan and transcatheter arterial chemoembolization in this study, and we use the anonymous clinical data during the analysis.

Conflict-of-interest statement: We have no financial relationships to disclose.

Data sharing statement: No additional data are available.

Correspondence to: Chuan-Dong He, MD, Associate Professor, Department of Radiology, Mianyang Central Hospital, 12 Changjia Road, Fucheng District, Mianyang 621000, Sichuan Province, China. hecd735@163.com
Telephone: +86-816-2222821

Received: November 3, 2015
Peer-review started: November 3, 2015
First decision: November 27, 2015
Revised: December 31, 2015
Accepted: January 17, 2016
Article in press: January 17, 2016
Published online: March 21, 2016

Abstract

AIM: To assess the value of gemstone spectral imaging (GSI) in efficacy evaluation in hepatocellular cancer (HCC) after transcatheter arterial chemoembolization (TACE) treatment.

METHODS: Thirty patients with HCC underwent GSI, including nonenhanced, arterial, portalvenous and delayed phase scans, after TACE treatment. Arterial phase images were acquired with GSI for reconstruction of virtual nonenhanced images and color overlay images. Digital subtraction angiography (DSA) was performed in all these patients. Two blinded and independent readers evaluated the data in two reading sessions; standard nonenhanced, arterial, portalvenous, and delayed phase images were read in session A, and the optimal monochromatic images, iodine/water based images and spectrum features were read in session B. Sensitivity and specificity were calculated with the DSA data as the reference standard. The sensitivity and specificity were compared using the χ^2 test.

RESULTS: DSA revealed 154 lesions in 30 patients, and 100 of them had blood supply. Overall sensitivity and specificity were 72% (72/100) and 77.8% (42/54) for session A, and 97% (97/100) and 94.4% (51/54) for session B, respectively. The sensitivity and specificity of the two reading sessions were significantly different (χ^2 = 23.04, χ^2 = 7.11, P < 0.05).

CONCLUSION: Compared with conventional CT, GSI could significantly improve the detection of small and multiple lesions without increasing the radiation dose. Based on spectrum features, GSI could assess tumor homogeneity and more accurately identify residual tumors and recurrent or metastatic lesions during efficacy evaluation and follow-up in HCC after TACE treatment.

Key words: Gemstone spectral imaging; Hepatocellular carcinoma; Transcatheter arterial chemoembolization; Digital subtraction angiography; Efficacy evaluation

Core tip: This is a retrospective study to evaluate the efficacy of gemstone spectral imaging (GSI) in hepatocellular cancer (HCC) after transarterial chemoembolization (TACE) treatment. The overall sensitivity and specificity of GSI in detection of lesions were 97% (97/100) and 94.4% (51/54), and 72% (72/100) and 77.8% (42/54) for conventional computed tomography (CT), respectively. Compared with conventional CT, GSI could not only significantly improve the detection of small and multiple lesions without increasing the radiation dose, but also could assess tumor homogeneity and more accurately identify residual tumors and recurrent or metastatic lesions during the follow-up in HCC after TACE treatment.

Liu QY, He CD, Zhou Y, Huang D, Lin H, Wang Z, Wang D, Wang JQ, Liao LP. Application of gemstone spectral imaging for efficacy evaluation in hepatocellular carcinoma after transarterial chemoembolization. *World J Gastroenterol* 2016; 22(11): 3242-3251 Available from: URL: http://www.wjgnet.com/1007-9327/full/v22/i11/3242.htm DOI: http://dx.doi.org/10.3748/wjg.v22.i11.3242

INTRODUCTION

Primary hepatocellular carcinoma (HCC) has an increasing incidence worldwide[1], and the incidence and mortality of HCC in China are both among the highest in the world[2]. The overall resectability rate of HCC is only 20%-30%, but the recurrence rate is as high as 60%-70%[3]. Currently, there are many non-surgical modalities for HCC, among which transcatheter arterial chemoembolization (TACE) is an effective method that has been widely used in clinical practice and become the first choice of non-surgical treatment[4]. The efficacy of TACE is closely associated with the extent of iodized oil deposition and tumor blood supply, and many HCC patients still have residual tumors after TACE. This, together with collateral vessel formation, results in the easy recurrence and metastasis of HCC. As a result, the majority of cases require repeated treatments[5]. Therefore, timely and accurate evaluation of TACE efficacy and early detection of active residual lesions and recurrent or metastatic lesions are of great clinical significance.

Many imaging modalities are currently available for efficacy evaluation and follow-up in HCC patients after TACE, including ultrasound, multislice computed tomography (MSCT), magnetic resonance imaging (MRI), positron emission tomography-computed tomography (PET-CT) and digital subtraction angiography (DSA)[6-9]. Each modality has its own pros and cons. DSA is the golden standard for the detection of viable tumors[10]; however, DSA is invasive and not suitable for routine monitoring. Therefore, there is still an urgent need to develop a simple, minimally invasive, effective and reproducible imaging modality for efficacy evaluation and follow-up in HCC patients after TACE.

In recent years, gemstone spectral imaging (GSI), which is able to comprehensively analyze the spectral characteristics of tumor lesions, has become a hot research topic in the fields of imaging and clinical oncology. As a novel imaging modality, GSI overcomes the limitation of conventional CT that adopts a single-parameter imaging mode relying on CT value only, and allows for the acquisition of polychromatic (QC) images, optimal monochromatic images, iodine (water)-based images, and spectral characterization diagrams by fast tube voltage switching (80/140 kVp) at one time, the generation of 101 monochromatic images at different kV levels from 40 to 140 keV, and the creation of multi-spectral images, thereby achieving multi-parameter imaging. Therefore, GSI achieves high-resolution imaging and material decomposition by qualitative and quantitative analysis, greatly improving the diagnostic accuracy and safety[10]. The present study assessed the value of GSI in efficacy evaluation and follow-up in HCC patients after TACE, with an aim to develop a simple, minimally invasive, effective and reproducible imaging modality for efficacy evaluation and early detection of active residual lesions and recurrent or metastatic lesions in HCC patients after TACE.

MATERIALS AND METHODS

Patients

Consecutive HCC patients who underwent TACE at our hospital from February 2013 to October 2014 were included. After excluding patients with cardiovascular or respiratory disease, poor renal function, allergy to contrast media, or contraindications for artery puncture, a total of 30 patients were finally included. There were 19 men and 11 women, and their age ranged from 36 to 72 years, with a mean value of 57.2 years. TACE was performed according to the standards for the diagnosis and treatment of primary liver cancer (updated in 2011). Follow-up and treatment interval were based on the same standards. The study protocol was approved by the local ethics committee, and all patients provided written informed consent prior to

TACE and GSI scans. The 30 patients received 1-3 TACE procedures, and GSI scans were performed 2-4 days before TACE treatment.

Examination procedures

Dual-phase GSI CT scans: A GE discovery CT750 HD CT scanner was used for plain and GSI CT scans. All patients were fasted for at least 8 h before the scans and took 800-1000 mL water before examination to fill the upper gastrointestinal tract to help identify the relationship between organs and avoid possible missed diagnosis of abdominal masses. The scanning range was from the dome of the diaphragm to the inferior poles of the two kidneys. After acquiring the scanogram, plain abdominal scanning was performed. The nonionic contrast medium iohexol (350 mg/mL, 80 mL) was then injected *via* the elbow vein at a flow rate of 2.9 mL/s. The amount of iohexol used for weak patients was calculated based on the body weight (kg), and the flow rate and the total amount of contrast medium were reduced correspondingly. The arterial and portal venous phase scans were started 35 s and 70 s after the start of injection of the contrast medium, respectively. Subsequently, the GSI mode was used to conduct dual-phase contrast enhanced scanning to acquire arterial and portal venous phase QC images and spectral images. Scan parameters included: voltage, 80/140 kVp; switching within 0.5 ms; default mA; helical pitch, 1.375:1; collimation width, 40 mm; slice thickness, 5 mm; reconstruction slice thickness, 1.25 mm and 0.625 mm.

DSA of the liver: Percutaneous femoral artery puncture was performed using the Seldinger technique. DSA of the celiac trunk, common hepatic artery, and superior mesenteric artery was performed. DSA images were acquired in the arterial, parenchymal, and venous phases. After determining tumor location, size, number and tumor-feeding arteries, the left hepatic artery, right hepatic artery, and tumor-feeding arteries were super-selectively catheterized with a microcatheter for infusion chemotherapy and embolization with iodized oil emulsion. The presence of active residual lesions and recurrent or metastatic lesions was judged based on the presence of enlarged tumor-feeding arteries, hypervascularity, tumor stain, and iodized oil deposition [standards for the diagnosis and treatment of primary liver cancer (updated in 2011)].

Image processing and evaluation

QC images and spectral images were acquired at one time of scan. Images were transferred to the AW4.6 workstation and processed using GSI-viewer software. One hundred and one monochromatic images at kV levels from 40 to 140 keV, iodine (water)-based images, and spectral characterization diagrams (spectral curve, scatter plot, *etc*.) were reconstructed. Based on the carrier-to-noise ratio (CNR), the images in which the lesion and adjacent liver tissue had the best CNR were selected from the 101 monochromatic images. The areas that had dense iodized oil deposition or radial artifacts should be avoided. On the QC images, optimal monochromatic images and iodine-based images, regions of interest (ROIs) of the same size were selected in the central slice of normal liver tissue and lesions in largest diameter to measure the CT value and effective iodine content and plot spectral characterization charts (spectral curve, scatter plot, *etc*.) to observe the characteristics of the spectral characterization charts (including slope of curve and distribution characteristics).

Two experienced radiologists who were blinded to the clinical details independently evaluated the status of tumor blood supply and the presence of active residual lesions and recurrent or metastatic lesions in two reading sessions (A and B), and the results were compared with DSA findings. For session A, QC images acquired in plain scans and in the arterial and venous phases (equivalent to conventional CT) were observed. For session B, optimal monochromatic images, iodine (water)-based images and spectral characteristics were observed. The consistency of the results of sessions A and B with DSA findings was evaluated. Discordant findings were resolved by consensus review by a third radiologist.

Statistical analysis

All statistical analyses were performed using SPSS17.0 software. Using DSA results as the reference golden standard, the sensitivity, specificity, positive predictive value, negative predictive value, and diagnostic coincidence rate for sessions A and B were calculated. The diagnostic performance between the two sessions was compared using the χ^2 test, and Kappa test was used to evaluate the consistency of the two sessions with DSA. P values < 0.05 were considered statistically significant.

RESULTS

Of the 30 HCC patients who underwent GSI examination after TACE treatment, 6 had single lesions and 24 had multiple lesions, as revealed by DSA. A total of 154 lesions were detected, and their diameter ranged from 1.1-14.4 cm (lesions that had an unclear boundary and fused together were counted as one). One hundred lesions had obvious hypervascularity and/or tumor stain, and 54 lesions only had iodized oil deposition without obvious tumor stain or hypervascularity (Figure 1A and B).

In session A, 84 lesions were identified to have enhancement, and 70 lesions had no enhancement. Seventy-two of the 84 lesions showing enhancement were correctly diagnosed, 12 lesions without blood supply were misdiagnosed as having enhancement, and 22 lesions having blood supply were missed.

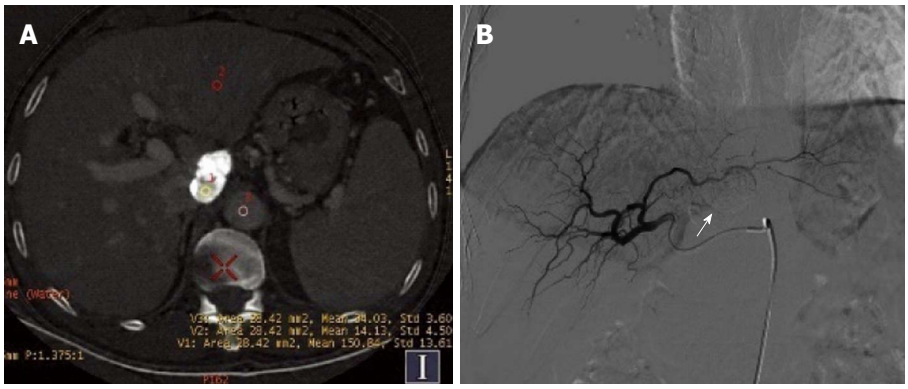

Figure 1 Hepatocellular cancer in the caudate lobe after transcatheter arterial chemoembolization. A: Iodine (water) based image. The effective iodine content of the defect of iodine deposition (154.10 ± 8.07) was significantly higher than that for normal liver parenchyma and the aorta (67.36 ± 4.87), revealing no residual tumor; B: Digital subtraction angiography image revealed no tumor vessels or stain, and obvious iodized oil deposition was visible (arrow).

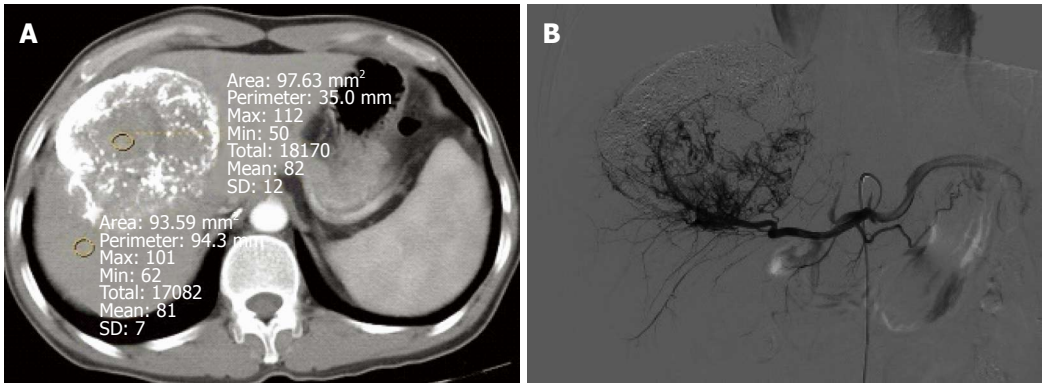

Figure 2 Giant hepatocellular cancer in the lateral borders of the left and right liver lobes after transcatheter arterial chemoembolization. A: The computed tomography (CT) value of the defect of iodine deposition was comparable to that of normal liver parenchyma in conventional CT image, and there was no obvious enhancement; B: Digital subtraction angiography revealed enlarged tumor blood vessels and tumor stain in the defect of iodine deposition.

Table 1 Numbers of lesions detected in sessions A and B and by digital subtraction angiography

DSA	A		B		Total
	With enhancement	Without enhancement	With enhancement	Without enhancement	
Abnormal tumor stain or tumor vessels	72	28	97	3	100
Iodized oil deposition only	12	42	3	51	54
Total	84	70	100	54	154

DSA: Digital subtraction angiography.

Twenty-two lesions were determined to have equidensity due to iodized oil artifact interference or cirrhotic background (Figure 2A and B), and 18 were misdiagnosed as cysts (Figure 3). Using DSA as the reference standard, the sensitivity, specificity, positive predictive value, negative predictive value, and diagnostic coincidence rate were 72% (72/100), 77.8% (42/54), 85.7% (72/84), 60% (42/70), and 74% (114/154), respectively (Table 1).

In session B, 100 lesions were identified to have enhancement (Figure 4A, B and C), and 54 lesions had no enhancement (Figure 5A, B and C). Ninety-seven of the 100 lesions showing enhancement were correctly diagnosed, three lesions without blood supply were misdiagnosed as having enhancement, and three lesions having blood supply were missed. The three lesions misdiagnosed to have enhancement were all located around areas of iodized oil deposition, and the six missed cases showed hypodensity and no enhancement, and were misdiagnosed as cysts (Figure 3). Using DSA as the reference standard, the sensitivity, specificity, positive predictive value, negative predictive value, and diagnostic coincidence rate were 97% (97/100), 94.4% (51/54), 97% (97/100), 94.4% (51/54), and 96.1% (148/154), respectively (Table 1).

In session B, CNR curve showed that the optimal monochromatic images were located at 60-70 KeV

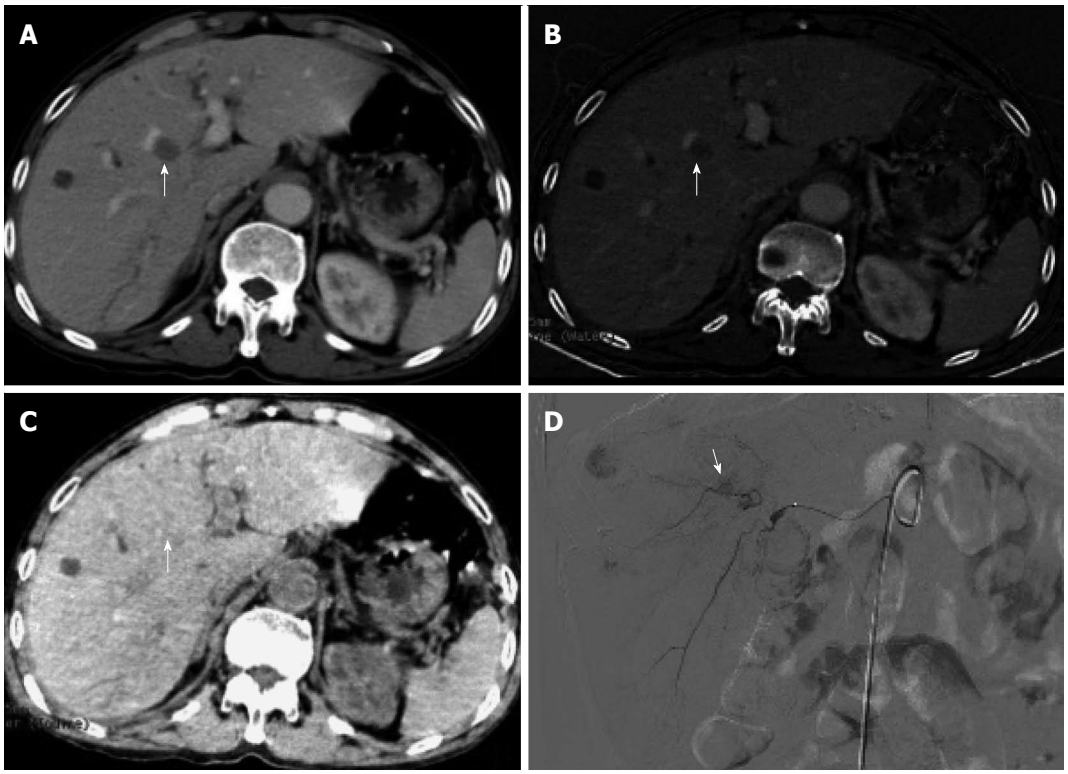

Figure 3 Metastasis to the medial segment of the left lobe of the liver after transcatheter arterial chemoembolization for primary hepatocellular cancer. A: Conventional computed tomography revealed that the left lobe metastasis had no obvious enhancement; B: Iodine (water) based image showed a small amount of contrast medium entry to the left lobe metastasis, suggesting slight enhancement; C: Iodine (water) based image showed equidensity of the left lobe metastasis; D: Digital subtraction angiography confirmed tumor stain in the left lobe metastasis in parenchymal phase (arrow).

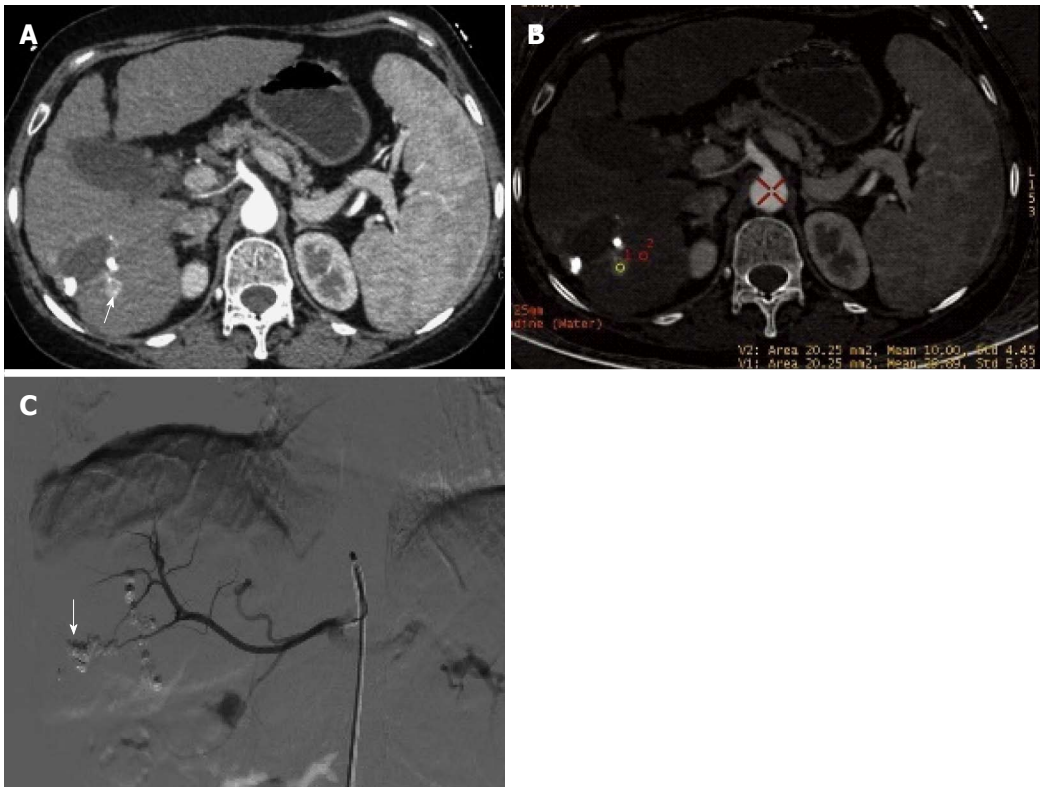

Figure 4 Recurrence of hepatocellular cancer in the right lobe after transcatheter arterial chemoembolization**.** A: Sixty-eight keV monochromatic image showed obvious enlargement and enhancement of recurrent lesion in tumor edge (arrow); B: The effective iodine content of the recurrent lesion (29.89 ± 5.83) was significantly higher than that for normal liver parenchyma (10.0 ± 4.45), suggesting obvious enhancement and entry of contrast medium to the lesion; C: Digital subtraction angiography confirmed tumor stain in the recurrent lesion in parenchymal phase (arrow).

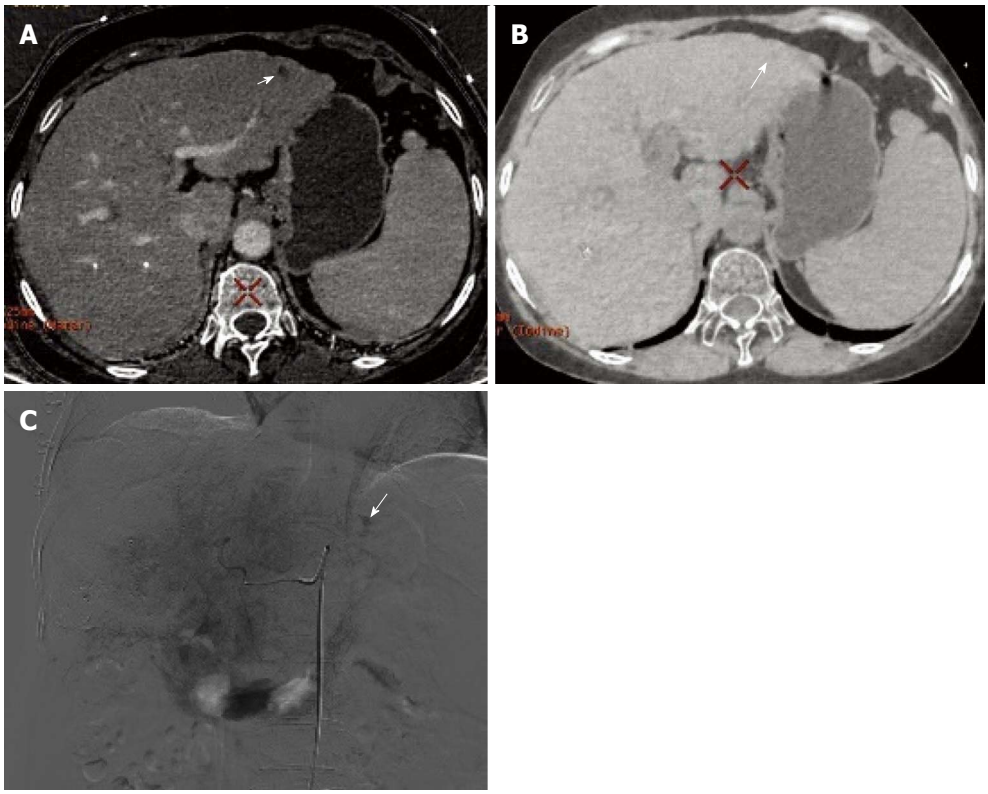

Figure 5 Same case as in Figure 4. A: Iodine (water) based image revealed no entry of contrast medium to the lateral segment of the left lobe, which showed hypodensity (arrow); B: Iodine (water) based image showed slight hypodensity (arrow); C: Digital subtraction angiography confirmed tumor stain in the left lobe metastasis in parenchymal phase (arrow).

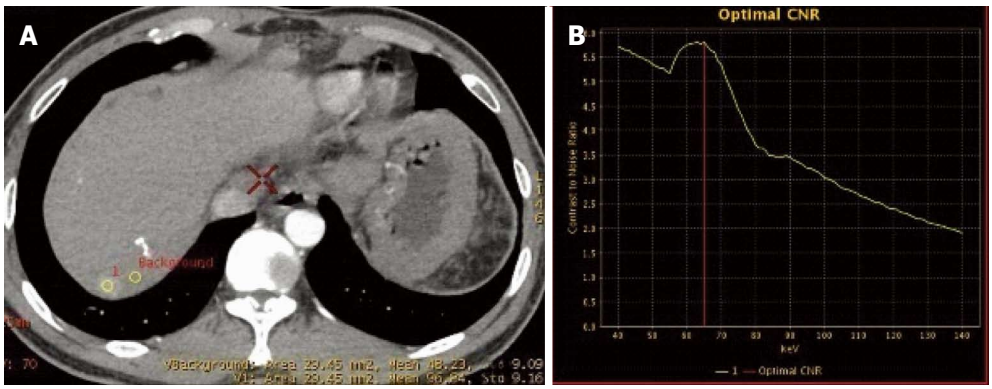

Figure 6 Metastasis to the right lobe after transcatheter arterial chemoembolization for hepatocellular cancer in the right lobe. A: Placement of regions of interest in the metastatic lesion and surrounding normal parenchyma, respectively; B: Carrier-to-noise ratio curve. The optimal monochromatic images were at 60-70 keV.

(Figure 6A and D). The slopes of spectral curves for post-treated lesions and pre-treated lesions were roughly identical and substantially overlapped (Figure 7A-D).

There were significant differences between the two sessions in sensitivity (χ^2 = 23.04, P < 0.01) and specificity (χ^2 = 7.11, P < 0.05). The consistency was moderate between session A and DSA (K = 0.47, P < 0.01), but good between session B and DSA (K = 0.91, P < 0.01).

DISCUSSION

Current status of efficacy evaluation in HCC after TACE

DSA can accurately detect tumor vessels, tumor stain, arteriovenous fistula and collateral circulation in active residual lesions after TACE treatment, and is therefore the most sensitive and specific method for evaluating the efficacy of TACE[11]. However, DSA is invasive, and postoperative monitoring relying on repeated DSA examinations is not practical. Currently,

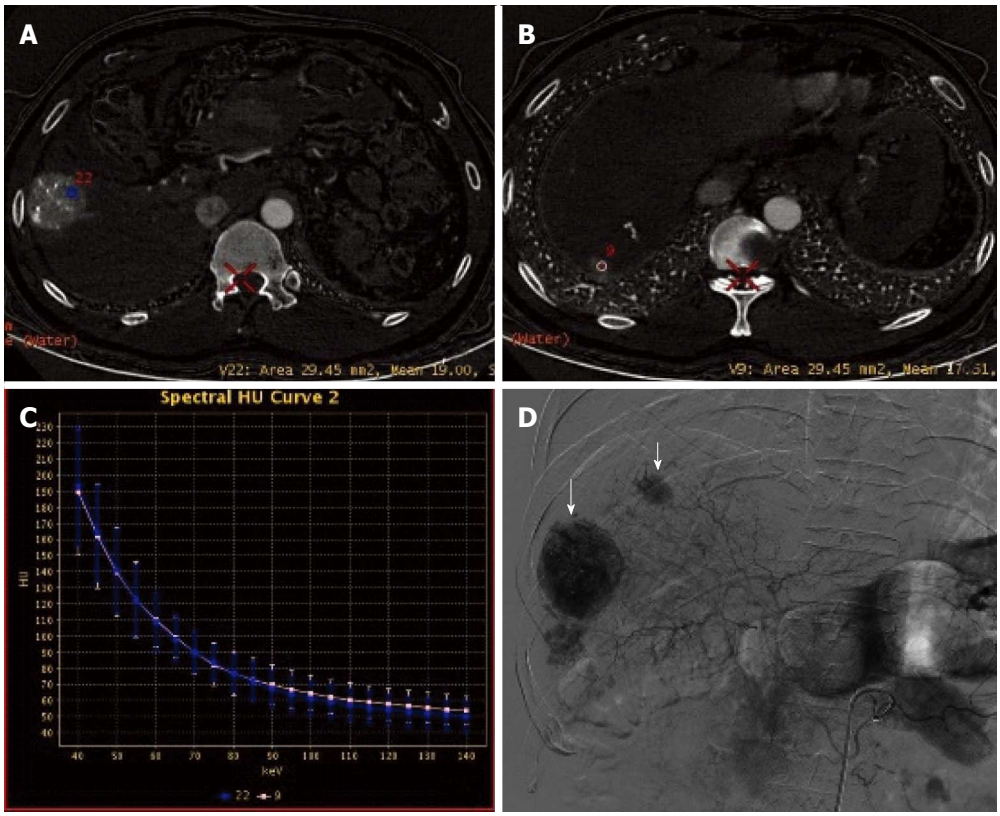

Figure 7 Same case as in Figure 6. A: Placement of a region of interest in the primary lesion; B: Placement of a region of interest in the lesion in the right lobe; C: The spectral curves for the two lesions were roughly same, suggesting tumor homogeneity; D: Digital subtraction angiography confirmed multiple tumor stains (arrow).

there are many imaging modalities available for efficacy evaluation in HCC after TACE, with CT and MRI being the main ones. MRI is not affected by iodized oil deposition, and it has been reported[12,13] that the sensitivity, specificity and accuracy of MRI are superior to those of CT and ultrasound; however, many contraindications and long scanning time limit its use. In addition, due to some overlap between DWI signals for viable tumor area and tumor necrotic area, it may be difficult to identify some residual tumors and lesions lacking rich blood supply. MSCT can better show the status of enhanced blood vessels and tumor blood supply in HCC, and it is the first choice of imaging modality for postoperative monitoring in HCC after TACE treatment[14,15]. However, conventional CT is based on mixed energy, can produce beam hardening artifacts, and cause the "drift" of CT value. Moreover, due to the impact of many other factors such as postoperative hemodynamic changes, uneven iodized oil deposition, radial artifacts around iodized oil deposition, degree of cell differentiation in lesions, non-rich arterial blood supply, arteriovenous double blood supply, and cirrhotic background, there may be poor contrast between lesions and the surrounding tissue. As a result, in some cases, conventional plain and contrast-enhanced CT scans may show equidensity or atypical enhancement pattern, thus weakening the ability of conventional CT to observe lesions around embolized lesions and evaluate residual tumor tissue, and decreasing the performance of CT in efficacy evaluation. In addition, due to the lack of blood supply in necrotic tumor tissue or the presence of coagulation necrosis after arterial embolization, defects of iodized oil deposition may be present. The defects of iodized oil deposition do not necessarily indicate the presence of residual tumors or recurrence[16]. Therefore, conventional CT has a low detection rate for small lesions and lesions lacking blood supply, and missed diagnosis is not uncommon[17]. During the process of evaluation of polychromatic images (equivalent to conventional CT) in this study, although ROIs were placed to avoid areas of dense iodized oil deposition and radial artifacts as far as possible, there were still 12 cases that were misdiagnosed as having enhancement due to reasons including iodized oil deposition. Of the 70 missed lesions, 28 were due to lack of blood supply without enhancement, 22 were identified to have equidensity due to iodized oil interference and cirrhotic background, and 18 were misdiagnosed as cysts.

Advantages and value of GSI in efficacy evaluation and follow-up in HCC after TACE

GSI adopts new high-purity and high-permeability detector materials, realizing fast kVp switching and single energy CT imaging. Therefore, GSI has obvious advantages and breakthroughs compared with conventional CT[18,19]. By optimizing the image quality

and choosing the optimal monochromatic images, GSI is conducive to eliminating beam hardening artifacts produced in conventional CT and avoiding average attenuation effect, thus increasing the contrast-noise ratio of images. Based on the difference in absorption coefficients of different materials under different single photon energy, GSI can also produce different characteristic absorption curves, thereby realizing the separation and identification of materials[20], *i.e.*, the spectral curves of different materials at different levels of KeV have different resolutions. Iodine based images can be used to directly determine iodine content and normalized iodine concentration, thereby indirectly reflecting blood supply status in different pathological conditions and in different stages of disease progression. Studies[21,22] have shown a significant correlation between the measured value and true value of iodine content in different concentrations of iodine-containing contrast medium, and that there was no significant difference between the measured value and true value. In the spectral curve for iodine, the difference between the CT values of iodine-containing hepatic artery and hepatic parenchyma increases with the decrease of the single energy KeV, thus improving the contrast between the lesions and normal liver tissue and the contrast between tissues, and exerting amplifying and highlighting effects. Therefore, GSI can, under the premise of without increasing radiation dose, improve the detection rate of lesions lacking blood supply, small lesions and multiple lesions, increase the qualitative accuracy, and avoid lesion missing[23-25], thus providing more robust information for accurate characterization, clear positioning, rapid diagnosis and timely treatment of diseases. In the present study, GSI showed that the optimal monochromatic images for lesions were at 60-70 KeV, and this finding is consistent with that reported in the literature[26]. The number of lesions detected by GSI was higher than that detected in polychromatic images (97 *vs* 72), and GSI findings had a good consistency with those of DSA. The sensitivity and specificity for the GSI group were significantly higher than those of the QC group. Three lesions showing enhancement in GSI were located around tumor lesions and iodized oil deposition areas, but DSA showed negative results. As non-nodular or non-mass lesions, their effective iodine contents and curve slopes were located between those for tumor lesions showing enhancement and normal parenchyma. We speculate that this may be due to reactive granulation tissue formation and/or iodized oil deposition after TACE for HCC. In this study, three lesions showed no enhancement in optimal monochromatic images by iodine quantitative measurement, but showed hypodensity in water (iodine)-based images. They were therefore misdiagnosed as cysts. Postoperatively, iodized oil deposition was visible, suggesting that they were metastases with no/little blood supply. In addition, conventional CT mainly observes the morphology of tumors and the change of CT values, but a significant change of tumor size often occurs 3 and 6 mo after chemotherapy[27]. GSI allows for analysis of the similarity of spectral characteristics between the pre-treated lesion and the post-treated lesion, thus providing objective information about the nature and origin of the lesion and aiding in the differential diagnosis[28-30]. In this study, it was found that the features of spectral curves and scatter plots for most of the detected lesions were substantially consistent with those for the pre-treated lesions, which suggests a homogeneity between them. However, there were few cases of inconsistency, and this was not caused by tumor cells themselves, but may be due to tumor liquefaction necrosis, few residual tumor cells, and many liquefaction necrosis foci in the ROIs.

Taken together, tumor morphological changes usually occur later than blood flow changes in HCC after TACE treatment, and therefore, morphological evaluation does not meet the requirements of efficacy evaluation. Compared to traditional CT value, effective iodine content in GSI has a higher correlation with iodine concentration, has a smaller error, can more accurately analyze material composition, can reflect real iodine concentration, and is more convincing. By measuring the amount of iodine accumulating in local tissue and comparing the change in the contents of iodine between pre-treated and post-treated lesions, GSI can indirectly reflect blood perfusion in tissues/organs and hemodynamic changes in lesions, and is therefore more sensitive and can detect more small lesions. By comparing the features of spectral characterization diagrams between suspicious lesions and primary lesions, GSI allows for more objective judgment and identification of residual lesions and recurrent or metastatic lesions, which is more accurate than conventional CT. However, this study has several limitations. Although a metal artifacts reduction system (MARS) was used in GSI, and areas of dense iodized oil deposition and radial artifacts were avoided as much as possible in the selection of ROIs in this study, some lesions were still misdiagnosed or missed due to iodized oil deposition; few lesions with no/little blood supply showing hypodensity in iodine (water) based images were misdiagnosed as cysts; the selection of size and placement of the ROIs were arbitrary, which may also lead to the change in the slopes of spectral curves. Therefore, future clinical studies are needed to address these issues carefully and optimize this technique.

GSI allows for multi-parametric imaging and overcomes the limitations of conventional CT, which relies on morphology and CT value and is a nonparametric imaging modality. Thus, GSI realizes the transition from morphological to functional imaging, and can therefore more accurately evaluate efficacy and detect active residual tumors and recurrent or metastatic lesions after TACE treatment for HCC, representing a simple, minimally invasive,

efficient imaging modality for efficacy evaluation and follow-up after TACE treatment for HCC. GSI also provides reliable imaging evidence for early treatment and is beneficial to the improvement of curative effect and survival.

COMMENTS

Background

The incidence and mortality of primary hepatocellular carcinoma (HCC) in China are both among the highest in the world. Because of its low resectable and high recurrent rates, transarterial chemoembolization (TACE) has been an effective non-surgical modality and widely used in clinical practice. However, many HCC patients still have residual tumors after TACE, which results in the easy recurrence and requires repeated treatments. Therefore, early detection of active residual lesions and recurrent or metastatic lesions after TACE are of great clinical significance. Although many imaging modalities are currently available for evaluation in HCC patients after TACE and among which DSA is the golden standard, it is invasive and not suitable for routine monitoring. In this study, we evaluate the efficacy of gemstone spectral imaging (GSI) in hepatocellular cancer after TACE.

Research frontiers

GSI has become a hot research topic in the fields of imaging and clinical oncology, for its ability to comprehensively analyze the spectral characteristics of tumor lesions without increasing the radiation dose at the same time. Few previous studies contain evaluations in HCC patients after TACE with GSI. The results of this study contribute to clarifying the potential of GSI for efficacy evaluation and follow-up in HCC patients after TACE.

Innovations and breakthroughs

In this study, GSI was a useful tool to detect the residual and recurrent or metastasis lesions of HCC after TACE. The sensitivity and specificity were 97% (97/100) and 94.4% (51/54), respectively. The results had a good consistency with those of DSA with a diagnostic coincidence rate of 74% (114/154) and were significantly higher than those of the QC group. This emphasizes the accuracy and efficacy of GSI for identifying residual tumors and recurrent or metastatic lesions.

Applications

This study suggests that GSI is useful for detecting the residual and recurrent or metastasis lesions of HCC after TACE. HCC patients after TACE can get timely and early further treatment if active residual lesions and recurrent or metastasis lesions are early and accurately detected based on the efficacy evaluation of the GSI.

Peer-review

As the authors indicated, the timely and accurate evaluation of TACE efficacy and early detection of active residual lesions and recurrent or metastatic lesions are of great clinical significance. In this manuscript, the authors assessed the value of gemstone spectral imaging in HCC after TACE treatment. The study is well designed and the results are interesting

REFERENCES

1 **Song do S**, Bae SH. Changes of guidelines diagnosing hepatocellular carcinoma during the last ten-year period. *Clin Mol Hepatol* 2012; **18**: 258-267 [PMID: 23091805 DOI: 10.3350/cmh.2012.18.3.258]

2 **Shi ZX**. Advances in imaging diagnosis of hepatocellular carcinoma. *Shiyong Fangshexue Zazhi* 2011; **27**: 784-787 [DOI: 10.3969/j.issn.1002-1671.2011.05.036]

3 **Llovet JM**, Bruix J. Novel advancements in the management of hepatocellular carcinoma in 2008. *J Hepatol* 2008; **48** Suppl 1: S20-S37 [PMID: 18304676 DOI: 10.1016/j.jhep.2008.01.022]

4 **Zangos S**, Gille T, Eichler K, Engelmann K, Woitaschek D, Balzer JO, Mack MG, Thalhammer A, Vogl TJ. [Transarterial chemoembolization in hepatocellular carcinomas: technique, indications, results]. *Radiologe* 2001; **41**: 906-914 [PMID: 11715582]

5 **Takayasu K**, Arii S, Ikai I, Omata M, Okita K, Ichida T, Matsuyama Y, Nakanuma Y, Kojiro M, Makuuchi M, Yamaoka Y. Prospective cohort study of transarterial chemoembolization for unresectable hepatocellular carcinoma in 8510 patients. *Gastroenterology* 2006; **131**: 461-469 [PMID: 16890600 DOI: 10.1053/j.gastro.2006.05.021]

6 **Minami Y**, Kudo M, Kawasaki T, Kitano M, Chung H, Maekawa K, Shiozaki H. Transcatheter arterial chemoembolization of hepatocellular carcinoma: usefulness of coded phase-inversion harmonic sonography. *AJR Am J Roentgenol* 2003; **180**: 703-708 [PMID: 12591679 DOI: 10.2214/ajr.180.3.1800703]

7 **Kim HC**, Kim AY, Han JK, Chung JW, Lee JY, Park JH, Choi BI. Hepatic arterial and portal venous phase helical CT in patients treated with transcatheter arterial chemoembolization for hepatocellular carcinoma: added value of unenhanced images. *Radiology* 2002; **225**: 773-780 [PMID: 12461260 DOI: 10.1148/radiol.2253011346]

8 **Bian DJ**, Xiao EH, Xiao YP, Chen XY, Situ WJ, He Z, Yuan SW, SunJN. MR perfusion imaging of the liver: early findings after transcantheter arterial chemoembolization of hepatocellular carcinoma. *Zhonghua Fangshexue Zazhi* 2010; **44**: 1248-1252 [DOI: 10.3760/cma.j.issn.1005-1201.2010.12.004]

9 **Peng LH**, Hu XY, Li J, Ding JR, Qiu DS, Zhang JT, Wei CJ. Clinicalapplication of 18F-FDG PET/CT imaging in detecting residual lesions or recurrence foci of hepatocellular carcinoma after TACE treatment. *Jieru Fangshexue Zazhi* 2012; **21**: 636-640 [DOI: 10.3969/j.issn.1008-794X.2012.08.006]

10 **Zheng XH**, Guan YS, Zhou XP, Huang J, Sun L, Li X, Liu Y. Detection of hypervascular hepatocellular carcinoma: Comparison of multi-detector CT with digital subtraction angiography and Lipiodol CT. *World J Gastroenterol* 2005; **11**: 200-203 [PMID: 15633215 DOI: 10.3748/wjg.v11.i2.200]

11 **Zhao LQ**, He W, Li JY, Chen JH, Wang KY, Tan L. Improving image quality in portal venography with spectral CT imaging. *Eur J Radiol* 2012; **81**: 1677-1681 [PMID: 21444170 DOI: 10.1016/j.ejrad.2011.02.063]

12 **Kubota K**, Yamanishi T, Itoh S, Murata Y, Miyatake K, Yasunami H, Morio K, Hamada N, Nishioka A, Ogawa Y. Role of diffusion-weighted imaging in evaluating therapeutic efficacy after transcatheter arterial chemoembolization for hepatocellular carcinoma. *Oncol Rep* 2010; **24**: 727-732 [PMID: 20664980]

13 **Kubota K**, Hisa N, Nishikawa T, Fujiwara Y, Murata Y, Itoh S, Yoshida D, Yoshida S. Evaluation of hepatocellular carcinoma after treatment with transcatheter arterial chemoembolization: comparison of Lipiodol-CT, power Doppler sonography, and dynamic MRI. *Abdom Imaging* 2001; **26**: 184-190 [PMID: 11178697]

14 **Zhuang GY**, Ren WX, Dili MB, GU JP.Evaluation of CT and DSA follow-up checkups forprimary hepatocellular carcinoma after transcatheter arterial chemoembolization: a comparative study. *Jieru Fangshexue Zazhi* 2009; **18**: 942-945 [DOI: 10.3969/j.issn.1008-794X.2009.12.018]

15 **Kim HJ**, Kim TK, Kim PN, Kim AY, Ko EY, Kim KW, Sung KB, Ha HK, Kim HC, Lee MG. Assessment of the therapeutic response of hepatocellular carcinoma treated with transcatheter arterial chemoembolization: comparison of contrast-enhanced sonography and 3-phase computed tomography. *J Ultrasound Med* 2006; **25**: 477-486 [PMID: 16567437]

16 **Zheng KG**, Xu DS, Li ZP, Quan XY. The correlation between "more hypodense areas" on CT scan and lipiodol deposition patterns of hepatic arterial lipiodol embolization in primary hepatoma. *Zhonghua Fangshexue Zazhi* 1995; **29**: 243-247

17 **Haider MA**, Amitai MM, Rappaport DC, O'Malley ME, Hanbidge AE, Redston M, Lockwood GA, Gallinger S. Multi-detector row helical CT in preoperative assessment of small (& lt; or = 1.5 cm) liver metastases: is thinner collimation better? *Radiology* 2002;

225: 137-142 [PMID: 12354997 DOI: 10.1148/radiol.2251011225]
18 **Lv P**, Lin XZ, Li J, Li W, Chen K. Differentiation of small hepatic hemangioma from small hepatocellular carcinoma: recently introduced spectral CT method. *Radiology* 2011; **259**: 720-729 [PMID: 21357524 DOI: 10.1148/radiol.11101425]
19 **Lin XZ**, Shen Y, Chen KM. Spectral CT imaging: principle, clinical application and research. *Zhonghua Fangshexue Zazhi* 2011; **45**: 798-800 [DOI: 10.3760/cma.j.issn.1005-1201.2011.08.028]
20 **Matsumoto K**, Jinzaki M, Tanami Y, Ueno A, Yamada M, Kuribayashi S. Virtual monochromatic spectral imaging with fast kilovoltage switching: improved image quality as compared with that obtained with conventional 120-kVp CT. *Radiology* 2011; **259**: 257-262 [PMID: 21330561 DOI: 10.1148/radiol.11100978]
21 **Graser A**, Johnson TR, Hecht EM, Becker CR, Leidecker C, Staehler M, Stief CG, Hildebrandt H, Godoy MC, Finn ME, Stepansky F, Reiser MF, Macari M. Dual-energy CT in patients suspected of having renal masses: can virtual nonenhanced images replace true nonenhanced images? *Radiology* 2009; **252**: 433-440 [PMID: 19487466 DOI: 10.1148/radiol.2522080557]
22 **Zhang D**, Li X, Liu B. Objective characterization of GE discovery CT750 HD scanner: gemstone spectral imaging mode. *Med Phys* 2011; **38**: 1178-1188 [PMID: 21520830]
23 **Wang GS**, Gao JH, Zhao S, Zhang XM, Mei Y. Comparing radiation dose and image quality between spectral CT and conventional multi-slice CT in imaging liver. *Zhonghua Fangshexue Zazhi* **2013**; 47: 340-343 [DOI: 10.3760/cma.j.issn.1005-1201.2013.04.011]
24 **Wang GS**, Gao JH, Zhao S. Clinical value of spectral CT for the detection of space occupying lesions in the liver. *Zhongguo Yixue Jisuanji Chengxiang Zazhi* 2013; **19**: 43-46 [DOI: 10.3969/j.issn.1006-5741.2013.01.011]
25 **Lv PJ**. Small hepatocellular carcinoma: detection with optimal monochromatic energy of spectral imaging. *Fangshexue Shijian* 2011; **26**: 321-324 [DOI: 10.3969/j.issn.1000-0313.2011.03.027]
26 **Ye XH**, Zhou C, Wu GG, Wang YY, Cao HZ, Shen Y. Primary study on the detection of hepatic tumors with spectral CT monochromatic imaging. *Zhonghua Fangshexue Zazhi* 2011; **45**: 718-722 [DOI: 10.3760/cma.j.issn.1005-1201.2011.08.003]
27 **Méndez Romero A**, Verheij J, Dwarkasing RS, Seppenwoolde Y, Redekop WK, Zondervan PE, Nowak PJ, Ijzermans JN, Levendag PC, Heijmen BJ, Verhoef C. Comparison of macroscopic pathology measurements with magnetic resonance imaging and assessment of microscopic pathology extension for colorectal liver metastases. *Int J Radiat Oncol Biol Phys* 2012; **82**: 159-166 [PMID: 21183292 DOI: 10.1016/j.ijrobp.2010.10.032]
28 **Lin XZ**, Li WX, Zhu YB, Dong HP, Lv PJ, Miao F, Li JY, Shen Y, Chen KM. Primary application of gemstone spectral imaging in the diagnosis of tumors. *Zhenduanxue Lilun Yu Shijian Zazhi* 2010; **9**: 155-160
29 **Yang L**, Wang SA, Zhu QQ, Wang J, Wang N. Spectral CT imaging in differentiation of liver small cysts from micro-metastatic lesions. *Zhongguo Yixue Shexiang Jishu* 2013; **29**: 92-96
30 **Yu YX**, Lin XZ, Chen KM, Chai WM, Hu SD, Tang RB, Zhang J, Cao LX, Rao YY, Yan FH. Values of spectral CT imaging in differential diagnosis of hepatocellular carcinoma and focal nodular hyperplasia. *Zhonghua Fangshexue Zazhi* 2013; **47**: 121-125 [DOI: 10.3760/cma.j.issn.1005-1201.2013.02.006]

P- Reviewer: Ehrhardt M, Tsai CA, Ugezu C
S- Editor: Ma YJ **L- Editor**: Wang TQ **E- Editor**: Liu XM

Published by **Baishideng Publishing Group Inc**
8226 Regency Drive, Pleasanton, CA 94588, USA
Telephone: +1-925-223-8242
Fax: +1-925-223-8243
E-mail: bpgoffice@wjgnet.com
Help Desk: http://www.wjgnet.com/esps/helpdesk.aspx
http://www.wjgnet.com

ISSN 1007-9327